



# CHORUS

This is the accepted manuscript made available via CHORUS. The article has been published as:

## Contracting non-Joulian magnets

Tanvir M. Saurav, Marcus L. Forst, James A. Boligitz, and Harsh Deep Chopra

Phys. Rev. B **95**, 174425 — Published 18 May 2017

DOI: [10.1103/PhysRevB.95.174425](https://doi.org/10.1103/PhysRevB.95.174425)

## Contracting non-Joulian magnets

Tanvir M. Saurav<sup>1</sup>, Marcus L. Forst<sup>1,2</sup>, James A. Boligitz<sup>1</sup>, and Harsh Deep Chopra<sup>1\*</sup>

<sup>1</sup>*Materials Genomics Laboratory, and Laboratory for Quantum Materials & Devices, Mechanical Engineering Department, Temple University, Philadelphia, PA, USA*

<sup>2</sup>*Physics Department, Temple University, Philadelphia, PA, USA*

\*Corresponding author. Email: [chopra@temple.edu](mailto:chopra@temple.edu)

**Abstract:** Recently, non-volume conserving or non-Joulian magnetostriction has been reported in Fe-Ga alloys [*Nature* **521**, 340 (2015); *ibid.*, **538** 416 (2016)] that *increase* their volume by expanding in magnetic fields. Here we report the complementary set of *contracting* non-Joulian crystals (Fe-Ge, Fe-Al) that decrease their volume. Results provide the critical compositional degree-of-freedom necessary for designing new alloys (beyond the initially reported Fe-Ga alloys) and establish this new family of functional materials based on non-Joulian magnetostriction.

## I. Introduction

Recent discovery of the non-Joulian magnetostriction (NJM) phenomenon in Fe-Ga alloys<sup>1,2</sup> expands the range of existing functional materials.<sup>3-8</sup> In contrast to Joule magnetostriction<sup>9</sup> in conventional magnets that is volume conserving,<sup>10,11</sup> the non-Joulian Fe-Ga alloys increase their volume by expanding in magnetic fields (e-NJMs). The possibility of contracting NJM or c-NJM (where volume decreases) also exists. Such a set of c-NJM alloys is reported here in Fe-Ge and Fe-Al alloys. Preliminary data on an Fe-Si based c-NJM alloy close to the cusp of zero-volume change (so-called ‘pivot’ or ‘master’ alloy) is also reported; it has a small but finite volume change and is not to be confused with conventional (Joule) magnets that are volume conserving.

## II. Experimental details

Potential non-Joulian alloys tend to show linear magnetization curves with practically zero hysteresis. The alloy compositions, Fe<sub>80.8</sub>Ge<sub>19.2</sub> and Fe<sub>67</sub>Al<sub>33</sub> (in at%), reported in this study exhibit these characteristics. Whereas the Fe<sub>80.8</sub>Ge<sub>19.2</sub> composition represents the peak in magnetostriction versus composition,<sup>12</sup> the properties of Fe-Al family of alloys in the vicinity of Fe<sub>67</sub>Al<sub>33</sub> are described elsewhere.<sup>13</sup> Also note that the composition of Fe<sub>83</sub>Al<sub>17</sub> corresponds to the peak in magnetostriction versus Al,<sup>12</sup> and single crystals of this composition are currently being grown.

Single crystals of Fe-Ge and Fe-Al were grown, heat-treated, oriented, and carved into discs at AMES Laboratory, IA. The discs were ~5 mm in diameter, ~1 mm thick, with the [001] crystal direction as the disc normal. The confirmation of single crystallinity is part of the elaborate crystal growth protocol at AMES Laboratory that includes repeated polishing and analysis in SEM. The orientation of the disc normal was accurate to 1°. Given the sensitivity of NJM to heat-treatments, the crystal growth process is described in detail here. High purity starting materials were arc-melted together into buttons several times under argon to form the base alloy. The buttons were then drop-cast into a copper mold. The drop-cast is placed in an alumina crucible and heated to just above the melting temperature under vacuum. The furnace is then back-filled with high-purity argon to a pressure of 40 psi to prevent volatilization, and held for 0.5 hour before continuing to heat until 150°C above the melting temperature of the alloy. The melt is held for 1 hour before withdrawing at a rate of 5 mm/hr. The as-grown ingots were annealed at 1000°C, unless there is a structural transition that should be avoided, in which case the ingot is annealed below this temperature. The ingot is cooled at a rate of 10 °C/min and this is referred to as the slow-cooled condition. Individually oriented samples may be additionally annealed at the same temperature as above by sealing them in quartz under a partial pressure of argon. The sample is put into a box furnace at a given temperature and held for 4 hours before quenching into water. This is referred to as heat-treated and quenched state. The annealing temperatures for Fe-Ge and Fe-Al were 770 °C and 1000 °C, respectively. Based on the similarities of the bulk magnetic properties (e.g., vector magnetization plots, NJM, etc.) of these alloys with Fe-Ga alloys, we expect a similar role of domains<sup>1</sup> in the manifestation of NJM, but micromagnetic studies are beyond the scope of this study.

Magnetostriction was measured by attaching strain gauges in a temperature-compensating Wheatstone bridge type setup (to minimize thermal drifts) using the lock-in amplifier technique

described previously.<sup>1, 14</sup> The resolution of our lock-in method is  $\sim 0.04\text{-}0.1$  ppm strain, and is typically  $< 0.1$  ppm. To measure strains normal to the discs, microstrain gauges were attached on the cylindrical surface of the sample, as described elsewhere.<sup>2</sup> Data was typically acquired at 100 scans/s and each point-by-point loop typically takes  $\sim 160$  s to measure. The scan rate is high enough to allow data points to be further averaged and smoothed. Vector magnetization measurements were performed using a high-resolution, low noise ( $5 \times 10^{-7}$  emu noise) vector vibrating sample magnetometer (VSSM from MicroSense) using real-time field control system. In the vector mode of a VSM, in addition to measuring the magnetization along the applied field (longitudinal component), component orthogonal to the field is also simultaneously measured.

### III. Results and Discussion

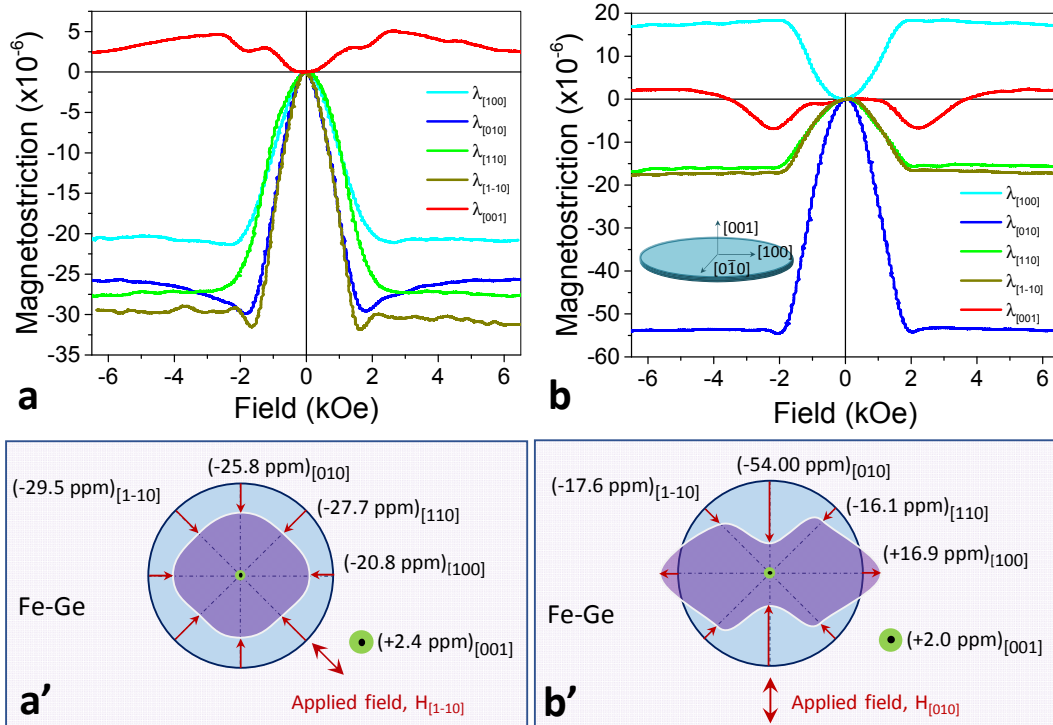


**Figure 1. Contracting NJM behavior of  $\text{Fe}_{80.2}\text{Ge}_{19.2}$  single crystal. a-a'**: Observed strains along different crystal axes when the applied field is along the in-plane,  $[1\bar{1}0]$  direction of the disc-shaped sample. The distortions (shown highly exaggerated) in **a'** use the various saturation magnetostriction values in **a** at 6.5 kOe, with reference to an initially circular disc. **b-b'**: Magnetostriction curves and schematic of the distortions along different directions for applied field along the in-plane  $[010]$  crystal axis.

Figure 1 shows the non-Joulian characteristics of a  $\text{Fe}_{80.2}\text{Ge}_{19.2}$  single crystal that was annealed at  $770^\circ\text{C}$  for 4 hours followed by water quenching. Figure 1a shows the various magnetostriction curves along different principal directions of the crystal when the applied field is along the in-plane,  $[1\bar{1}0]$  crystal axis; Fig. 1a' schematically shows the distortions (exaggerated) of the initially circular disc. Similarly, Fig. 1b-b' shows the observed magnetostriction curves and

distortions when the field is along the in-plane [010] axis. Also notice that each magnetostriction curve in Fig. 1 saturates, including the curve along the [001] direction.

When the applied field is along the  $[1\bar{1}0]$  axis, Fig. 1a-a', the sample decreases its volume by radially contracting in an almost isotropic manner (radial strains range from -21 to -30 ppm), while simultaneously experiencing only a negligible expansion normal to the disc that saturates at +2.4 ppm. In contrast, the crystal distortions are anisotropic when the applied field is along the [010] direction, as shown in Fig. 1b-b'. In this case, the crystal exhibits a large longitudinal contraction of -54 ppm along the [010] axis, which, along with contractions along the two in-plane  $\langle 110 \rangle$ -type directions (between -16 to -17 ppm), vastly offset the in-plane transverse expansion of +16.9 ppm along the [100] direction as well as the miniscule (+2.0 ppm) expansion normal to the disc, for a net volume decrease.

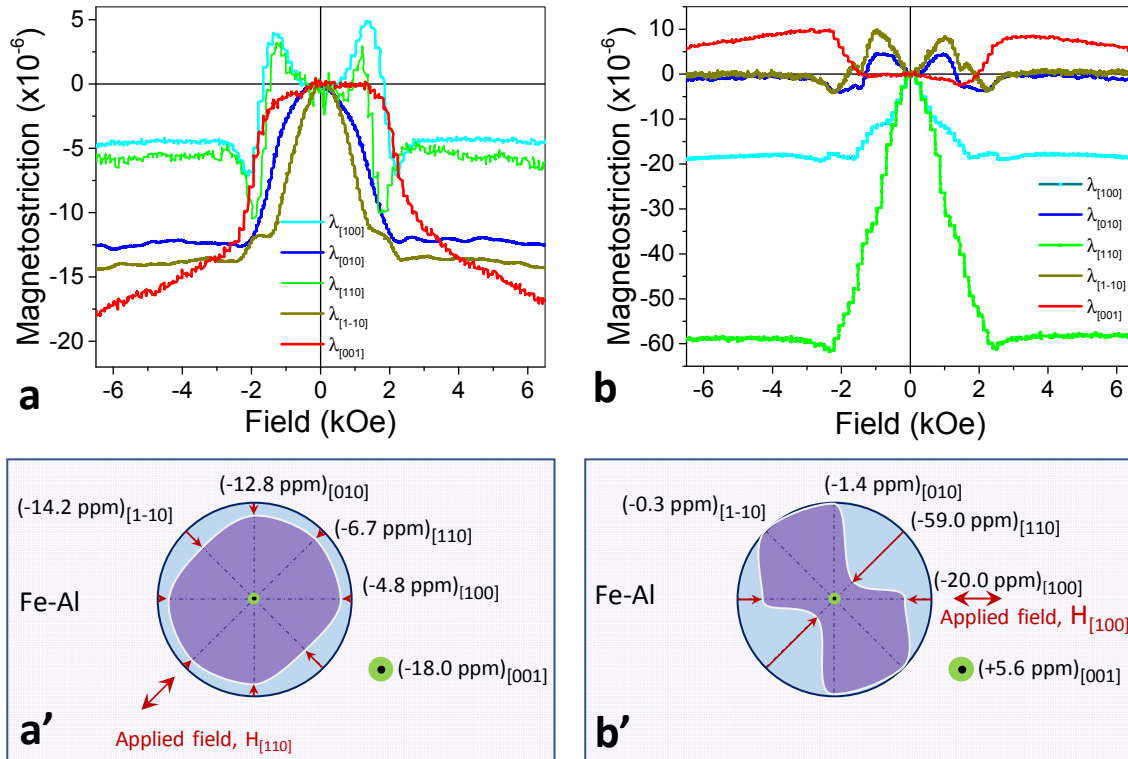


**Figure 2. Contracting NJM behavior of  $\text{Fe}_{67}\text{Al}_{33}$  single crystal. a-a'**: Observed strains along different crystal axes when the applied field is along the in-plane  $[110]$  direction of the disc-shaped sample. The distortions shown in a' use the various saturation magnetostriction values in a at 6.5 kOe (except for the  $[001]$  direction where magnetostriction was measured up to  $\sim 8.5$  kOe). **b-b'**: Magnetostriction curves and distortions along different directions for applied field along the in-plane  $[100]$  crystal axis.

Similarly, Fig. 2a-a' (field along the  $[110]$  axis) and 2b-b' (field along the  $[100]$  axis) shows the c-NJM behavior in a  $\text{Fe}_{67}\text{Al}_{33}$  single crystal. Like the Fe-Ge crystal in Fig. 1a-a', the Fe-Al crystal also contracts radially when the field is directed along the  $[110]$  direction (but is less

isotropic). Moreover, it also contracts significantly along the disc normal (-18.0 ppm), for a net volume decrease. For applied field along the [100] direction, the maximum magnetostriction is much higher (-59 ppm) in comparison to the distortions when the field is along the [110] direction.

Figure 3a-b shows the field dependence of the relative volume change ( $\delta V/V_0$ ) as well as the absolute volume change ( $\delta V$ ) for the Fe-Ge and Fe-Al single crystals, respectively. These plots were obtained by first averaging the radial diameters at selected fields, using the curves shown in Fig. 1a and Fig. 2a. Figure 3 clearly establishes the contracting nature of these non-Joulian crystals (the more cumbersome volume calculations associated with applied field along the  $\langle 100 \rangle$  type direction in Fig. 1b or 2b are not plotted).

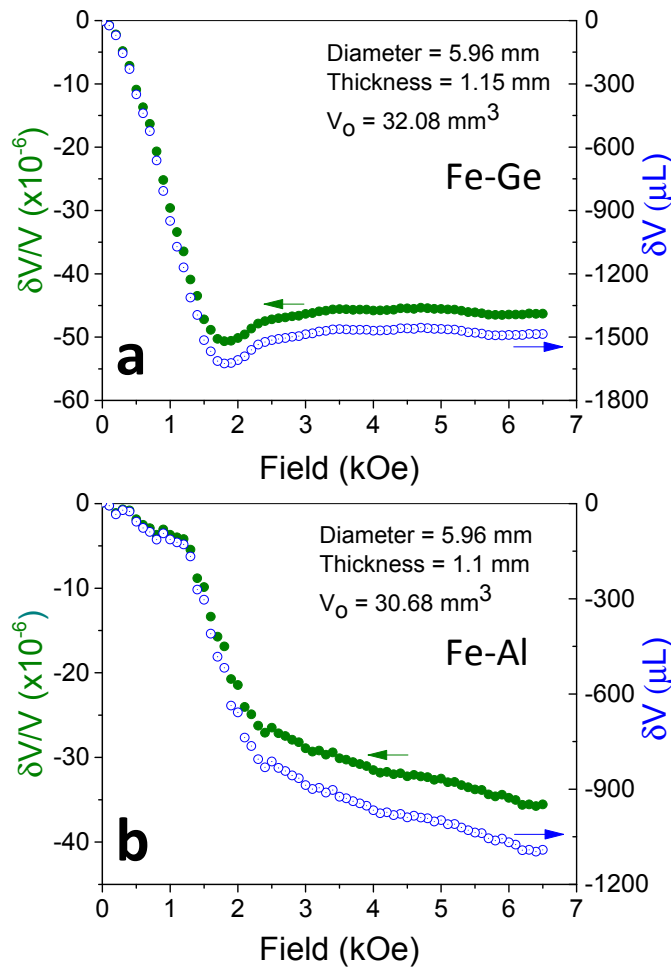


**Figure 3. Contracting nature of Fe-Ge and Fe-Al non-Joulian crystals. a,** Relative and absolute volume change in Fe-Ge single crystals with applied field along the  $[1\bar{1}0]$  direction, corresponding to Fig. 1a-a', and **b,** in Fe-Al single crystal with applied field along the  $[110]$  direction, corresponding to Fig. 2a-a'. The sample dimensions for the two crystals are also shown.

Common to all non-Joulian crystals is the observation of linear magnetization versus field (M-H) curves regardless of the crystal direction in which they are measured. Linear M-H curves for Fe-Ga, Fe-Al, and Fe-Ge were previously discussed.<sup>1</sup> Our new precision measurements reveal the exceptional nature of the linearity, see Fig. 4a and its lower-right inset, as well as their hysteresis-free state (upper-left inset of Fig. 4a), using Fe-Al. This behavior, including the isotropy of magnetization, is unprecedented for crystalline magnets. Figure 4a shows that the coercivity of the crystal along various in-plane directions is essentially non-existent (0.5 mOe). However, in a narrow range of angles (outside the range shown in Fig. 4a, not shown) the angular dependence of coercivity is found to abruptly change from essentially non-zero in Fig. 4a to a finite but small value,  $\sim 0.12$  Oe or 0.27 Oe, and this behavior is currently being further investigated.

The orthogonal vector component of magnetization (in-plane,  $M_y$ ) was simultaneously measured along with the longitudinal magnetization,  $M_x$ , at different static fields. Results show that the amplitude of  $M_y$  becomes maximum, Fig. 4b, at a field that coincides with onset of saturation magnetostriction in each alloy. (The component of magnetization normal to the disk,  $M_z$  was also measured but is negligible and not discussed further). For example, the maximum value of  $M_y$  approaches 20-25% of  $M_x$  for the quenched Fe-Ga alloy described in Ref. [1]). When the *absolute value* of maximum magnetostriction for various alloys is plotted as a function of the observed maxima in  $M_y$ , Fig. 4c, the resulting data shows an exponential curve fit.

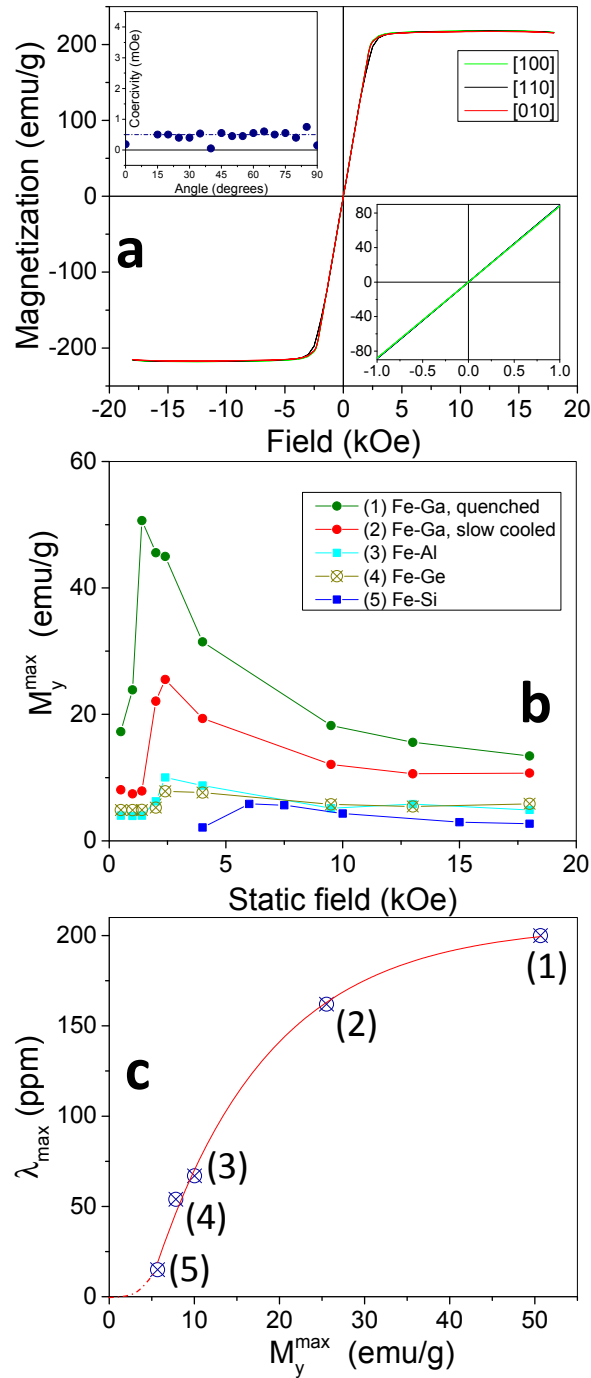


**Figure 4: Common features of non-Joulian magnets.** **a:** Highly linear, hysteresis-free and isotropic magnetization curves along different in-plane directions of the disc-shapes Fe-Al crystal. Although not shown, magnetization curves were measured every  $5^\circ$  and were found to be virtually isotropic. The upper-left inset shows that hysteresis is non-existent (0.5 mOe) along various directions. The lower-right inset highlights the linearity of the curves. **b:** Amplitude of the in-plane, transverse vector component of magnetization ( $M_y$ ) as a function of static field in

different crystals. For each alloy the peak in  $M_y$  coincides with the onset of saturation magnetization and magnetostriction. **c**: Absolute value of maximum magnetostriction in various alloys versus their respective peak value of  $M_y$  (from **b**). The red curve fit shows an exponential dependence of  $\lambda_{\max}$ .

In Fig. 4b-c, also notice the inclusion of an Fe-3.1wt%Si alloy. This alloy was subject to a long-term aging treatment, following which it exhibits features similar to other non-Joulian magnets (including linearly reversible and isotropic magnetization). This non-Joulian crystal also shows a small but definitive volume decrease. Its detailed behavior is being discussed elsewhere.<sup>15</sup> Its near-zero volume change puts it close to the cusp or crossover from e-NJM to c-NJM, the significance being that it represents the ‘master’ alloy for designing ternary or even quaternary alloys with control over their magnitude and/or sign of non-Joulian response.

The significance of the plot in Fig. 4c is that it unifies the behavior of all contracting and expanding non-Joulian alloys, as seen from the observed exponential fit to the absolute value of maximum magnetostriction that is independent of the composition of the iron-based alloys (Fe with Ga, Ge, Al, or Si) or prior thermal treatment (quenched or slow cooled Fe-Ga). To explain, for the volume of any crystal to change, the interatomic distances must change necessarily. Previously, the non-Joulian behavior was attributed to the existence of an elastically modulated structure<sup>1</sup> whose origin was proposed to be charge density waves (CDWs).<sup>16</sup> Using nanoscale Scanning X-ray Diffraction Microscopy (nano-SXDM)<sup>17, 18</sup> complemented by element-specific soft x-ray magnetic circular dichroism photoemission electron microscopy (XMCD-PEEM),<sup>19, 20</sup> we have recently shown the existence of long-wavelength (~270 nm) lattice modulations and a corresponding magnetic modulation of similar periodicity (~255 nm) in the quenched Fe-Ga crystal.<sup>21</sup> It is found that the resulting elastic-magnetic coupling produces a bulk strain that is equal to the directly measured self-strain across the periodic elastic modulations, and attributed to field-induced unfolding of the modulated elastic structure to produce a volume change. The existence of an internally heterogeneous state is also reflected in the field dependence of  $M_y$ , Fig. 4b, which peaks and then decrease to a saturation value; by contrast, the  $M_y$  component in conventional magnetic approaches zero at saturation and beyond. The decrease in amplitude of  $M_y$  beyond the respective maxima in Fig. 4b for various alloys signifies a progressive saturation in the unfolding of the heterogeneous state within the crystal. In this proposed model, a small value of  $M_y$  is associated with a small self-strain of the modulation, and likewise, a large value of  $M_y$  with a larger self-strain. Eventually, there has to be an upper elastic limit to the self-strain associated with lattice modulation, which represents the exponential approach to saturation in Fig. 4c.

To conclude, the full set of contracting and expanding non-Joulian magnets increases the compositional degree of freedom needed to design new (ternary, quaternary, etc.) alloys with control over the magnitude and sign of NJM, as well as conceiving new magnetic invars that conserve volume. Together with the previously reported Fe-Ga alloys, results establish the new class of functional materials based on NJM.

## Acknowledgments

H.D.C. gratefully acknowledges the support of the National Science Foundation DMR-Condensed Matter Physics grant 1541236, and Temple University Merit Scholars Grants to J.A.B, M.L.F. and T.M.S. Magnetization and magnetostriction measurements were designed by H.D.C. and done by M.L.F., T.M.S., and H.D.C. Single crystal of the iron-based alloys were synthesized at the Materials Preparation Center, AMES Laboratory, USDOE; see [www.mpc.ameslab.gov](http://www.mpc.ameslab.gov). Correspondence and requests for materials should be addressed to H.D.C. ([chopra@temple.edu](mailto:chopra@temple.edu)).

## References

1. H. D. Chopra and M. Wuttig, *Nature* **521** (7552), 340-343 (2015).
2. H. D. Chopra and M. Wuttig, *Nature* **538** (7625), 416-416 (2016).
3. E. K. H. Salje, *Chemphyschem* **11** (5), 940-950 (2010).
4. A. Sozinov, A. A. Likhachev, N. Lanska and K. Ullakko, *Applied Physics Letters* **80** (10), 1746-1748 (2002).
5. S. Guruswamy, N. Srisukhumbowornchai, A. E. Clark, J. B. Restorff and M. Wun-Fogle, *Scripta Materialia* **43** (3), 239-244 (2000).
6. R. D. James and M. Wuttig, *Philosophical Magazine A* **77** (5), 1273-1299 (1998).
7. H. D. Chopra, C. H. Ji and V. V. Kokorin, *Physical Review B* **61** (22), 14913-14915 (2000).
8. A. E. Clark and H. S. Belson, *Physical Review B* **5** (9), 3642-& (1972).
9. J. P. Joule, *On the Effects of Magnetism upon the Dimensions of Iron and Steel Bars. The London, Edinburgh and Dublin philosophical magazine and journal of science.* (Taylor & Francis 30, Third Series: 76–87, 225–241, 1847).
10. É. du Trémolet de Lacheisserie, D. Gignoux and M. Schlenker, *Magnetism Fundamentals.* (Springer, Grenoble Sciences France).
11. C.-W. Chen, *Magnetism and Metallurgy of Soft Magnetic Materials.* (Elsevier, Amsterdam: North-Holland, 1977).
12. J. B. Restorff, M. Wun-Fogle, K. B. Hathaway, A. E. Clark, T. A. Lograsso and G. Petculescu, *Journal of Applied Physics* **111** (2), 023905 (2012).
13. R. D. Shull, H. Okamoto and P. A. Beck, *Solid State Communications* **20** (9), 863-868 (1976).
14. M. Sullivan, *Review of Scientific Instruments* **51** (3), 382-383 (1980).
15. H. D. Chopra, M. L. Forst and T. M. Saurav, unpublished (2017).
16. G. Grüner, *Density Waves in Solids.* (Perseus Publishing, Cambridge, Massachusetts, 2000).
17. M. Holt, R. Harder, R. Winarski and V. Rose, *Annual Review of Materials Research* **43** (1), 183-211 (2013).

18. T. T. A. Lummen, Y. Gu, J. Wang, S. Lei, F. Xue, A. Kumar, A. T. Barnes, E. Barnes, S. Denev, A. Belianinov, M. Holt, A. N. Morozovska, S. V. Kalinin, L.-Q. Chen and V. Gopalan, *Nature Communications* **5**, 3172 (2014).
19. A. Doran, M. Church, T. Miller, G. Morrison, A. T. Young and A. Scholl, *Journal of Electron Spectroscopy and Related Phenomena* **185** (10), 340-346 (2012).
20. A. T. Young, E. Arenholz, J. U. N. Feng, H. Padmore, S. Marks, R. Schlueter, E. Hoyer, N. Kelez and C. Steier, *Surface Review and Letters* **09** (01), 549-554 (2002).
21. W. Yang, R. U. Chandrasena, M. L. Forst, J. A. Boligitz, A. Arab, M. V. Holt, A. Scholl, E. Arenholz, H. Ebert, J. Minár, T. A. Lograsso, A. X. Gray and H. D. Chopra, *Science* (2017 in review).